

# Mode filtering based on ponderomotive force nonlinearity in a plasma filled rectangular waveguide

H SOBHANI<sup>1</sup>, H R SABOUHI<sup>2</sup>, S FEILI<sup>3</sup> and E DADAR<sup>4</sup>

<sup>1</sup>Young Researchers and Elite Club, Qom Branch, Islamic Azad University, Qom, Iran

<sup>2</sup>Department of Electrical Engineering, Hormoz Branch, Islamic Azad University, Hormoz Island, Iran

<sup>3</sup>Department of Physics, Shahid Bahonar University, Kerman, Iran

<sup>4</sup>Faculty of Economic, Mofid University, Qom, Iran

E-mail: [H\\_sabouhi@yahoo.com](mailto:H_sabouhi@yahoo.com)

Received 11 May 2017, revised 18 July 2017

Accepted for publication 18 July 2017

Published 23 August 2017



CrossMark

## Abstract

Here a new scheme for mode filtering is proposed. Based on the ponderomotive force effect, propagation of the microwave dual-mode through a plasma-filled metallic rectangular waveguide is investigated. To excite the  $TE_{20}$  mode in a rectangular waveguide, the existence of fundamental modes is unavoidable. To filter the destructive mode ( $TE_{10}$ ), the waveguide is filled with a collisional plasma. Based on the coupling effect, the energy of this destructive  $TE_{10}$  mode is transferred to the  $TE_{20}$  mode. The proposed structure acts like a mode convertor. The  $TE_{10}$  mode become more attenuated and instead the  $TE_{20}$  mode is amplified. The plasma filled rectangular waveguide acts as a mode filtering tool.

Keywords: mode filtering, mode convertor, collisional plasma, ponderomotive force

(Some figures may appear in colour only in the online journal)

## 1. Introduction

Recent progression in wireless communication systems has created a need for tools such as the microwave (MW) multiplexers, waveguide filters and RF circuits, which have reduced the production cost and compact size [1–4]. Waveguides are usually constructed so that only one mode propagates, while sometimes the existence of other modes is unavoidable. In rectangular waveguide, the  $TE_{10}$  mode is the dominant mode. To provoke the  $TE_{20}$  mode, the wave frequency is greater than its cutoff frequency, so the existence of fundamental modes is unavoidable. The existence of  $TE_{10}$  mode is modified in the electron density distribution. To have a higher order mode (such as  $TE_{20}$  mode) without the destructive mode (such as  $TE_{10}$  mode) a some research has been investigated. Recently, a substrate integrated waveguide (SIW) slot array antenna with a  $TE_{20}$  mode to realize bore-sight radiation was proposed [5]. Also, the excitation of two wideband  $TE_{20}$  mode is surveyed by a novel SIW structure [6]. In other methods, a mode converter has been proposed

[7]. In this converter, the energy of this destructive  $TE_{10}$  mode is used to amplify the  $TE_{20}$  mode. Furthermore, by using a nonlinear plasma and choosing the suitable initial conditions, a method to convert Hypergeometric-Gaussian subfamily mode to one or more mode components of Laguerre-Gaussian modes has been demonstrated [8]. Here we proposed that to filter destructive mode, the waveguide can be filled with a nonlinear plasma. Based on this proposed structure, the energy of this destructive  $TE_{10}$  mode is transferred to the  $TE_{20}$  mode. By the ponderomotive force nonlinearity, the  $TE_{10}$  mode is attenuated and instead the  $TE_{20}$  mode is amplified, therefore our structure is a mode convertor. On the other hand, due to filter the destructive mode, a mode filtering occurred in the our plasma waveguide structure. Recently, a waveguide structure based on embedding a graphene film for spatial-mode-filtering applications has been proposed [9]. In other work, the ability of periodic sub-wavelength grating waveguides to use for mode filtering is investigated [10]. The utility of the plasma for filtering has been applied in other research. A photonic crystal doped by

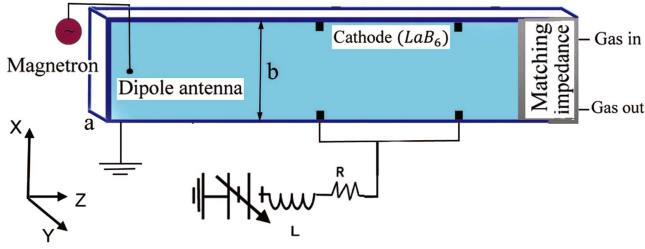


**Figure 1.** The  $TE_{10}$  and  $TE_{20}$  modes of the evacuated metallic waveguide, with the width  $a = 2$  cm and height  $b = 1$  cm, are provoked by a magnetron through a dipole antenna. By employing an electric discharge between  $LaB_6$  cathode and the waveguide grounded surfaces, the plasma is produced in the right-hand waveguide [26].

plasma has been surveyed to filter the defect mode of the TE wave [11]. Wave-plasma interaction leads to many interesting phenomena, such as resonance absorption [12–14], wave generation [15–19], frequency shift [20] and modification of electron density distribution [8]. Such types of interaction are active fields of research due to their broad range of applications in the areas like MW reflectometry, stellarators, controlled fusion, RF-based plasma thrusters and plasma production [21–25]. One of the important nonlinear occurrences in the high MW propagation in plasma is the ponderomotive force effect. In the presence of ponderomotive force, the charged particles, such as electrons, are expelled from regions of high field strength. The electron density modification in the plasma by the ponderomotive force of strong-power MW has been investigated [26]. Propagating high power MW in a plasma-filled metallic waveguide has been surveyed [23, 27].

In section 2, propagating high-power MW dual-mode in an evacuated waveguide that provokes a plasma filled in a similar and co-axis waveguide is investigated. The effect of coupling on each modes via the ponderomotive force through a collisional plasma is surveyed. Section 3 is devoted to study the propagation and evolution of  $TE_{10}$  and  $TE_{10}$  modes in rectangular waveguide. Finally, the conclusion is presented in section 4.

## 2. Device modeling and analysis

In this section, a mode filtering tool based on the plasma filled rectangular waveguide is demonstrated. A scheme of an evacuated rectangular waveguide, which is connected coaxially to an plasma filled waveguide, is presented in figure 1. The waveguides have similar sizes (1 cm  $\times$  2 cm). A dipole antenna provokes the  $TE_{10}$  and  $TE_{20}$  modes in the evacuated metallic waveguide [28]. To produce plasma in the second waveguide, we employed an electric discharge between  $LaB_6$  cathodes [13] and the waveguide grounded surfaces. Here, the effects of plasma and  $LaB_6$  cathodes on the modes is ignored. By choosing the wave frequency greater than the  $TE_{20}$  cutoff frequency, the  $TE_{20}$  mode excites in the rectangular waveguide. The cutoff frequency of  $TE_{20}$  mode is higher than that of  $TE_{10}$ , so the fundamental modes is provoked. When the excited  $TE_{10}$  and  $TE_{20}$  modes encounter plasma, the characteristics of the

modes are varied. The cutoff frequency of the modes in the plasma waveguide is greater than that of the evacuated waveguide. Thus the modes propagate with larger wavelength into the plasma filled waveguide. The existence of  $TE_{10}$  mode modified the plasma, which varied the propagating characteristic of  $TE_{20}$  mode. The incidence of a strong MW on the plasma is supposed perpendicularly. Recently, the governing equations of the MW field propagation through the plasma-filled rectangular waveguide has been demonstrated [26].

The permittivity of the collisional plasma can be expressed as  $\epsilon'_0 + i\epsilon'_i + \Phi(\mathbf{E} \cdot \mathbf{E}^*)$ , where  $\epsilon'_0(z) = 1 - \frac{\omega_p^2(z)}{\omega^2 + \nu_{ei}^2}$ ,  $\epsilon'_i(z) = \frac{\nu_{ei}}{\omega} \frac{\omega_p^2(z)}{\omega^2 + \nu_{ei}^2}$ ,  $\Phi$  is the nonlinear effect, which created by the ponderomotive force,  $\omega$  is the MW frequency and  $\nu_{ei}$  is the electron-ion collision frequency [29–31]. Also,  $\omega_p = \left(\frac{e^2 n_0}{\epsilon_0 m_e}\right)^{1/2}$  is the plasma frequency where  $n_0$ ,  $\epsilon_0$ ,  $m_e$  and  $e$  are the equilibrium electron density, vacuum permittivity, electron mass and electron charge, respectively. Here,  $\mathbf{E}$  is the sum of electric fields of  $TE_{10}$  and  $TE_{20}$  modes. Due to absorption in collisional plasma, the wavenumber is imaginary as  $k(z) = k_r(z) + ik_i(z) = \frac{\omega}{c} [\epsilon'_0(z) + i\epsilon'_i(z)]^{1/2}$ , where  $c$  is the velocity of light,  $k_r(z)$  is the wavenumber of MW beam, and  $k_i(z)$  is related to the MW energy damping rate. By propagating the MW in plasma, the ponderomotive force accelerates the electron, which creates a lower electron density. The ponderomotive force exerted on the ions is ignored. It is assumed that the plasma pressure gradient force is lower than the ponderomotive force. Therefore, the nonlinearity term is expressed as  $\Phi(\mathbf{E} \cdot \mathbf{E}^*) = \frac{\omega_p^2}{\omega^2 + \nu_{ei}^2} (1 - e^{-\eta \mathbf{E} \cdot \mathbf{E}^*})$ , where  $\eta = e^2 / (8m_e \omega^2 k_B T_0)$ ,  $T_0$  and  $k_B$  are the equilibrium temperature of plasma and Boltzmann constant, respectively [27, 31]. The electron density, modified by the ponderomotive force, may be written as  $n_0 = n_{00} e^{-\eta \mathbf{E} \cdot \mathbf{E}^*}$ , where  $n_{00}$  and  $n_0$  are the electron density in the absence and presence of the MW electric field, respectively [8, 27]. The dielectric permittivity varies as a function of the sum of electric fields of  $TE_{10}$  and  $TE_{20}$  modes, which is considered as  $E_{1y}(x, y, z) = E_{10}(z) \sin(\pi x/a) e^{i(\int k(z) dz - \omega t)}$  and  $E_{2y}(x, y, z) = E_{20}(z) \sin(2\pi x/a) e^{i(\int k(z) dz - \omega t)}$ . The electric fields of modes separate out as  $E_{10}(z) = A_r(z) + iA_i(z)$  and  $E_{20}(z) = B_r(z) + iB_i(z)$ . The separated amplitudes are substituted in the MW field propagation equation through the plasma-filled rectangular waveguide (which is demonstrated in [27]). Then the real and imaginary parts of the MW field propagation equation are separated for each mode and some mathematical manipulations are employed. By multiplying both sides of the MW field propagation equation by  $\sin(n\pi x/a)$  and integrating over  $x$  (0 to  $a$ ), the variation of separated amplitudes are written as

$$\frac{\partial^2 A_r}{\partial z^2} - 2k_i \frac{\partial A_i}{\partial z} + 2k_r \frac{\partial A_r}{\partial z} - \frac{\partial k_i}{\partial z} A_i + \frac{\partial k_r}{\partial z} A_r - \left(\frac{\pi}{a}\right)^2 A_r + \frac{\omega^2}{c^2} \Phi(\mathbf{E} \cdot \mathbf{E}^*) A_r = 0 \quad (1a)$$

$$\frac{\partial^2 A_i}{\partial z^2} + 2k_i \frac{\partial A_r}{\partial z} + 2k_r \frac{\partial A_i}{\partial z} + \frac{\partial k_i}{\partial z} A_r + \frac{\partial k_r}{\partial z} A_i - \left(\frac{\pi}{a}\right)^2 A_i + \frac{\omega^2}{c^2} \Phi(\mathbf{E} \cdot \mathbf{E}^*) A_i = 0 \quad (1b)$$

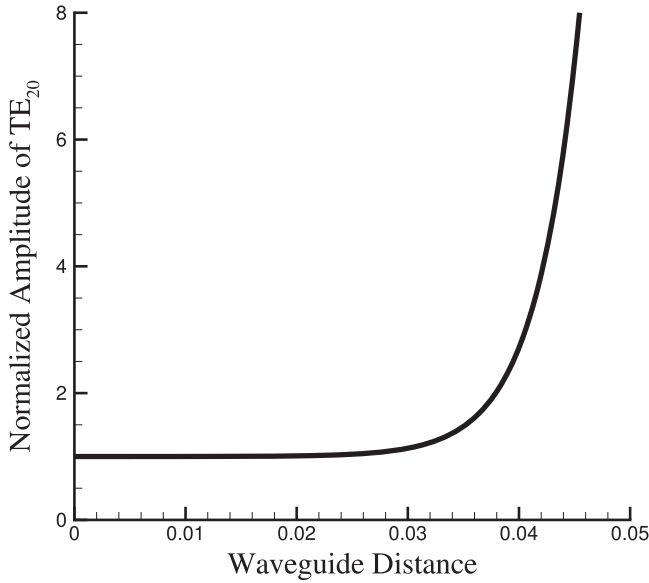


**Figure 2.** Normalized amplitude of TE<sub>20</sub> mode versus the distance  $z$  (m) in the plasma-filled waveguide.

$$\frac{\partial^2 B_r}{\partial z^2} - 2k_i \frac{\partial B_i}{\partial z} + 2k_r \frac{\partial B_r}{\partial z} - \frac{\partial k_i}{\partial z} B_i + \frac{\partial k_r}{\partial z} B_r - \left(\frac{2\pi}{a}\right)^2 B_r + \frac{\omega^2}{c^2} \Phi(\mathbf{E} \cdot \mathbf{E}^*) B_r = 0 \quad (1c)$$

$$\frac{\partial^2 B_i}{\partial z^2} + 2k_i \frac{\partial B_r}{\partial z} + 2k_r \frac{\partial B_i}{\partial z} + \frac{\partial k_i}{\partial z} B_r + \frac{\partial k_r}{\partial z} B_i - \left(\frac{2\pi}{a}\right)^2 B_i + \frac{\omega^2}{c^2} \Phi(\mathbf{E} \cdot \mathbf{E}^*) B_i = 0. \quad (1d)$$

Equations (1a)–(1d) are coupled together. The coupling effect of modes is clear in the nonlinear term as  $\mathbf{E} = E_{1y}\hat{j} + E_{2y}\hat{j}$ , where  $\hat{j}$  is the unit vector in the  $y$ -direction. Considering the boundary condition for metallic waveguide, the coupled equations (1a)–(1d) are solved numerically. When the energy relaxation time of electrons ( $t \ll \tau_e = \frac{M}{2m_e\nu_{ei}}$ ), where  $M$  is the ion mass, is larger than the time duration of MW, the ponderomotive nonlinearity is dominant [29].

To derive equations (1a)–(1d), orthogonality relations between  $\sin(\pi x/a)$  and  $\sin(2\pi x/a)$  is employed. The orthogonality relations of  $\sin(n\pi x/a)$  is written as

$$\int_0^a \sin(n\pi x/a) \sin(m\pi x/a) dx = \frac{a}{2} \delta_{n,m}. \quad (2)$$

### 3. Results and discussion

Considering the boundary condition for the metallic waveguide, the spatial distribution of electric fields is varied as equations (1a)–(1d). The MW frequency should not be selected too close to the cutoff frequency, since the conductor losses are then large [28]. The MW frequency is 20 GHz, so the TE<sub>10</sub> and TE<sub>20</sub> modes can excite in the waveguide. Parameters are taken as  $L = 0.05$  m,  $\omega_p = 0.9$  GHz,  $\nu_{ei} = 0.05 \omega_p$  and the MW intensity  $I = 2 \times 10^8$  W/m<sup>2</sup>.

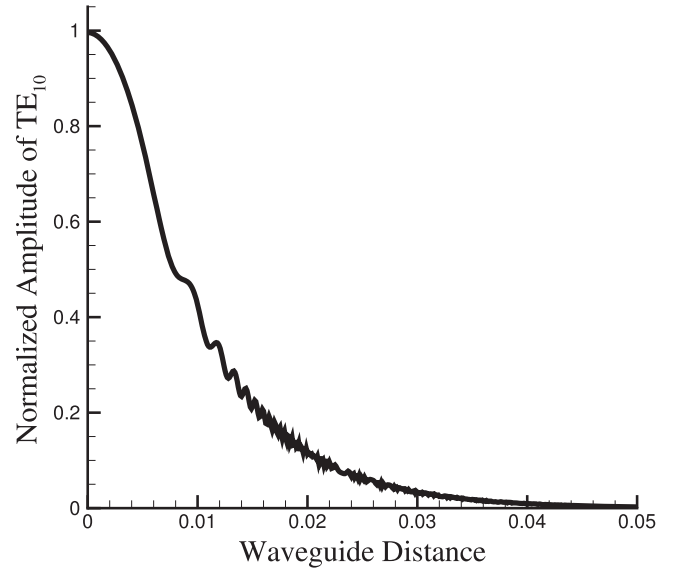
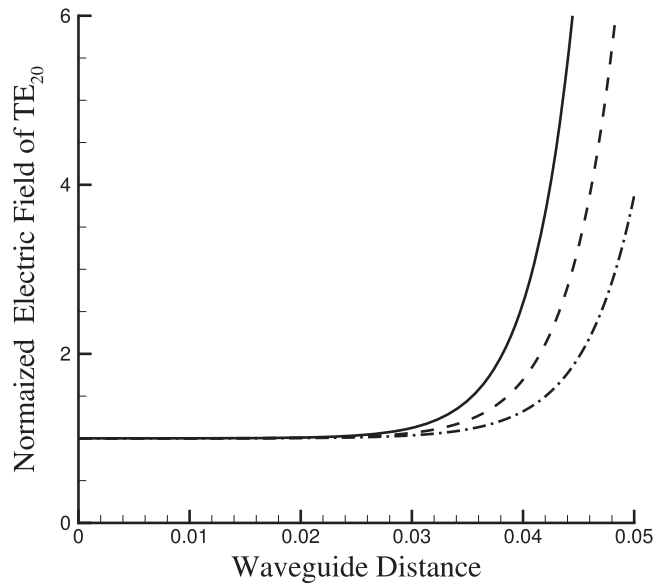


**Figure 3.** Normalized amplitude of TE<sub>10</sub> mode versus the distance  $z$  (m) in the plasma-filled waveguide.

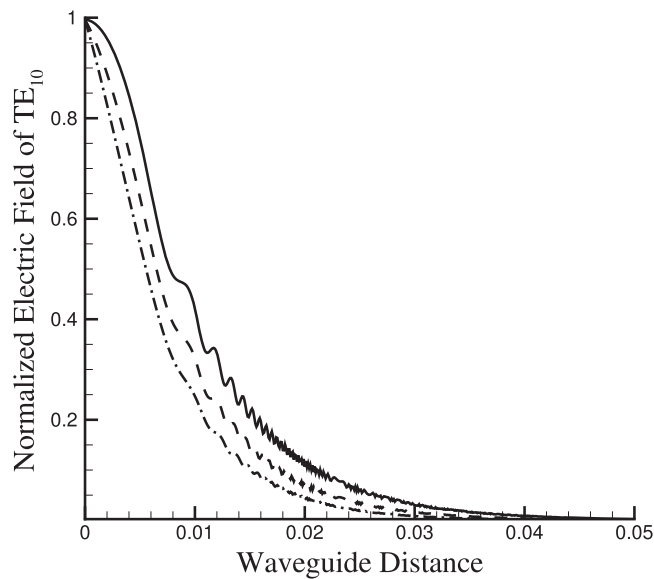
In figure 2, the normalized amplitude of electric field for TE<sub>20</sub> mode ( $\sqrt{B_r(z)^2 + B_i(z)^2}$ ) in collisional plasma is presented. As maintained above, the electrons are repulsed from high intensity regions by the ponderomotive force. Hence at the location of  $a/2$  for the TE<sub>10</sub> mode and  $a/4$  &  $3a/4$  for TE<sub>20</sub> mode, the dielectric permittivity is raised. The outset of the propagation path at  $a/2$  of the waveguide width, the TE<sub>10</sub> mode has high intensity, so the ponderomotive force accelerates the electrons to a location of  $a/4$  and  $3a/4$ . When the plasma frequency grows, the ponderomotive force nonlinearity increases. The plasma plays the role of a convex lens and converging the MW takes place. The normalized amplitude of TE<sub>20</sub> mode is increased. However the plasma is collisional so the normalized amplitude of the TE<sub>20</sub> mode is slowly attenuated. The growth of electric field amplitude due to the nonlinearity is challenged to the attenuation due to collisional absorption. Finally, the ponderomotive force nonlinearity is predominated and the normalized amplitude of electric field is increased.

Figure 3 illustrates the normalized amplitude of electric field for the TE<sub>10</sub> mode ( $\sqrt{A_r(z)^2 + A_i(z)^2}$ ) in the plasma waveguide. By rising the normalized amplitude of the TE<sub>20</sub> mode, the electron density at a location of  $a/2$  decreases and is larger near the waveguide walls. Plasma plays the role of a concave lens, so the effect of diffraction occurs and MW diverges. At a location of  $a/2$ , the plasma frequency and ponderomotive force nonlinearity decrease. Due to the collisional attenuation and diffraction effect, the normalized amplitude of TE<sub>10</sub> attenuates. By selecting the higher collision frequency, the decreasing rate of the normalized amplitude takes place rapidly. So the collision frequency can be considered as a controlled parameter.

Furthermore, the observed result can be described by the energy conservation law. By propagating the TE<sub>10</sub> and TE<sub>20</sub> modes in the proposed waveguide, this structure acts like a



**Figure 4.** Normalized electric field of TE<sub>20</sub> mode versus the distance  $z$ (m), when the collision frequency is  $\nu_{ei} = 0$  (solid line),  $0.05\omega_p$  (dashed line) and  $0.1\omega_p$  (dash-dotted line) in the plasma-filled waveguide.



**Figure 5.** Normalized electric field of TE<sub>10</sub> mode versus the distance  $z$ (m), when the collision frequency is  $\nu_{ei} = 0$  (solid line),  $0.05\omega_p$  (dashed line) and  $0.1\omega_p$  (dash-dotted line) in the plasma-filled waveguide.

mode filtering tool. The TE<sub>20</sub> mode is amplified and the TE<sub>10</sub> mode is filtered. On the other hand, the energy transfers from the TE<sub>10</sub> mode to the TE<sub>20</sub> mode.

In the presence of the electron-ion collision, the electromagnetic energy of modes is absorbed via collision. To survey the collision effect in collisional plasma, the normalized electric field of TE<sub>20</sub> mode ( $\sqrt{B_r(z)^2 + B_i(z)^2} e^{-\int k_i(z) dz}$ ), which is attenuated by the collision effect for three different collision frequencies, is presented in figure 4. The more the collision frequency is selected, the lower amplification of the

normalized electric field for the TE<sub>20</sub> mode occurs. In figure 5, the normalized electric field of the TE<sub>10</sub> mode ( $\sqrt{A_r(z)^2 + A_i(z)^2} e^{-\int k_i(z) dz}$ ), which is attenuated by the collisional effect for three different collision frequencies, is pictured. As seen, the more the collision frequency is selected, the higher absorption of the normalized electric field takes place.

#### 4. Conclusion

A method to filter the destructive mode on the basis of ponderomotive force nonlinearity is proposed. To suppress the fundamental mode, a collisional plasma-filled waveguide is designed. This aim is provided by surveying a mode filtering that is based on amplifying the TE<sub>20</sub> mode and filtering the TE<sub>10</sub> mode. Based on the ‘coupling effect’, the energy of this destructive TE<sub>10</sub> mode is transferred to the TE<sub>20</sub> mode. On the other hand, this proposed structure is a mode convertor. To clarify the collision effect in this structure, the effect of exchange in collision frequency on the electric field of modes is investigated. Finally, this structure is useful to many industrial and technological applications.

#### Acknowledgments

This work was supported by Hormoz branch, Islamic Azad University, Iran, Hormoze Island grant. We also thank the faculty members at the electrical engineering department for their cooperation and for being welcoming during the project.

#### References

- [1] Liu J C *et al* 2010 *IEEE Microw. Wirel. Compon. Lett.* **20** 142
- [2] Mokhtaari M *et al* 2006 *IEEE Trans. Microw. Theory Tech.* **54** 3940
- [3] Rosenberg U *et al* 2003 *IEEE Trans. Microw. Theory Tech.* **51** 1735
- [4] Kunes M 1998 *Electron. Commun. Eng. J.* **10** 29
- [5] Xu J *et al* 2011 A single-layer SIW slot array antenna with TE<sub>20</sub> mode *Asia-Pacific Microwave Conference Proceedings (APMC)* (Melbourne: IEEE) 1330
- [6] Wu P *et al* 2015 *IEEE Trans. Microw. Theory Tech.* **63** 1863
- [7] Kokubo Y *et al* 2010 *Microw. Opt. Technol. Lett.* **52** 169
- [8] Sobhani H *et al* 2017 *Opt. Laser Technol.* **81** 40
- [9] Chang Z *et al* 2016 Mode filter based on graphene-embedded waveguide *Optical Fiber Communication Conference, Optical Society of America* (Anaheim, CA: Optical Society of America) Th3E-6
- [10] Galacho D *et al* 2015 Mode filtering in periodic waveguides by means of band gap engineering *Optical Interconnects Conference (OI)* (San Diego, CA: IEEE) 68
- [11] Kong X K *et al* 2010 *Phys. Plasmas* **17** 103506
- [12] DiVergilio W F *et al* 1977 *Phys. Rev. Lett.* **38** 541
- [13] Rajyaguru C *et al* 2001 *Phys. Rev. E.* **64** 016403
- [14] Lee Y *et al* 1986 *Phys. Fluids* **29** 3785
- [15] Sobhani H *et al* 2016 *J. Phys. D Appl. Phys.* **49** 295107
- [16] Sobhani H *et al* 2016 *Eur. Phys. J. D* **70** 168
- [17] Sobhani H *et al* 2017 *Phys. Plasmas* **24** 023110
- [18] Sobhani H *et al* 2017 *J. Plasma Phys.* **83** 655830101

- [19] Sobhani H 2017 *Twisted Terahertz Generation Carrying Angular momentum in plasma Effective Factors* (Saarbrücken: LAP LAMBERT Academic) <https://amazon.com/Twisted-Terahertz-Generation-Carrying-momentum/dp/333007471X>.
- [20] Xu X *et al* 1997 *Phys. Rev. E* **55** 3328
- [21] Kamal-Al-Hassan M D *et al* 2003 *Phys. Rev. E* **68** 036404
- [22] Jawa S K *et al* 2005 *Opt. Commun.* **25** 346
- [23] Malik H K *et al* 2010 *J. Appl. Phys.* **108** 013109
- [24] Godyak V *et al* 2001 *Plasma Sources Sci. Technol.* **10** 459
- [25] Ito H *et al* 2004 *Phys. Rev. E* **69** 066406
- [26] Niknam A R *et al* 2013 *Waves Random Complex Media* **23** 183
- [27] Sobhani H *et al* 2016 *Waves Random Complex Media* **1** 1
- [28] Harrington R F 1961 *Time-Harmonic Electro Magnetic Fields* (New York: McGraw-Hill)
- [29] Sodha M S *et al* 1974 *Self-Focusing of Laser Beams in Dielectrics, Plasmas and Semiconductors* (New Delhi: MacGraw-Hill)
- [30] Sodha M S *et al* 1976 *Prog. Opt.* **13** 169
- [31] Faisal M *et al* 2007 *Phys. Plasmas* **14** 103103